Bistability and squeezing of the librational mode of an optically trapped nanoparticle

Ke-Wen Xiao,[1] Nan Zhao,[1] and Zhang-qi Yin[2,*]
[1]Beijing Computational Science Research Center, Beijing 100193, China
[2]Center for Quantum Information, Institute for Interdisciplinary Information Sciences, Tsinghua University, Beijing 100084, China
(Received 9 May 2017; published 19 July 2017)

We systematically investigate the bistable behavior and squeezing property of the librational mode of a levitated nonspherical nanoparticle trapped by laser beams. By expanding the librational potential to the fourth order of the librational angle θ, we find that the nonlinear coefficient of this mode is dependent only on the size and material of nanoparticle, but independent of trapping potential shape. The bistability and hysteresis are displayed when the driving frequency is red detuned to the librational mode. In the blue-detuned region, we have studied squeezing of the variance of librational mode in detail, which has potential application for measurement of angle and angular momentum.

DOI: 10.1103/PhysRevA.96.013837

I. INTRODUCTION

Enormous research progress in quantum optomechanics has been reported in the past few years [1,2]. Applications in metrology, such as ultrasensitive detectors for force sensing [3,4], millicharge searching [5], and other uses [6–8], have been studied. When the motion is cooled to the quantum ground state, it can be utilized for the detection of quantum gravity [9] and the test of objective collapse models [10]. There are many different optomechanical systems, such as microtoroid [11], near-field coupled nanomechanical oscillators [12], and optical microsphere resonator [13]. At the same time, an optically levitated nanoparticle in vacuum begins to show its potential as a novel optomechanical system [14–17], which has ultra-high-quality factor $Q > 10^9$ [16,18]. Therefore, it can be applied for ultrasensitive measurement [17,19], such as in the measurement of force [7], torque [20], and mass [21], and for testing the boundary between quantum and classical mechanics [22–25].

A levitated nanoparticle has three translational modes and three rotational modes. Much theoretical and experimental progress has been reported, such as the measurement of instantaneous velocity of a Brownian particle [17], the cooling of translational mode of nanoparticle [15,16,26,27], and so on. Meanwhile, the librational (torsional) mode attracts more and more attention. However, these theoretical investigations were based on utilizing multiple Laguerre-Gaussian cavity modes [14,28,29] or microwindmills [30]. In Refs. [31,32], the directions of the optically levitated dielectric nanoparticles were fixed, and the librational (torsional) optomechanics of a levitated nonspherical nanoparticle was reported. In these experiments, the torsional mode of an ellipsoidal nanoparticle levitated by a linearly polarized Gaussian beam was experimentally observed, and the scheme of a sideband cooling torsional mode was proposed [31]. Inspired by these experiments, researchers studied the decoherence mechanism of optically trapped nanoparticle librational modes [33,34], coupling librational modes with the internal spins [35–37], etc.

The nonlinearity of optomechanical systems offers rich new physics in both classical and quantum regimes [38–44], and many investigations and applications of nonlinear optomechanical systems have been reported, such as ultrasensitivity optical sensor [45], cooling by utilising nonlinearity [46], and observation of bistability in a macroscopic mechanic resonator from a single chemical bond [47]. The nonlinearity of a translational mode is usually very small and therefore can be neglected. In this paper, we systematically investigate the nonlinearity of the torsional mode of a levitated nonspherical nanoparticle. We find that the nonlinearity is independent of the amplitude and frequency of the trapping laser, but depends only on the inertia of the nanoparticle. The nonlinearity could be very large when the size of the particle is small. The system can show bistability by driving the librational mode. It is worth mentioning that the red-detuning driving laser causes bistability of torsional mode, and the blue-detuning laser does not. By carefully tuning the driving detuning, the librational mode could be prepared into the squeezed state and be used for the precision measurements of the angle and the angular momentum.

This paper is organized as follows. In Sec. II, we theoretically investigate the nonlinear effect of the librational mode of a nonspheric nanoparticle trapped by laser beams and deduce its Hamiltonian. In Sec. III, we study the steady state of this nonlinear system and find that librational modes have bistability. In Sec. IV, we derive the linearized Hamiltonian and study the squeezing property of this system. In the last section, Sec. V, we give a brief conclusion and perspective.

II. MODEL

As show in Fig. 1, we consider one librational mode of an optically levitated ellipsoidal nanoparticle with long axis r_a, short axis $r_b = r_c$, and density ρ. For simplicity, we suppose that all other degrees of freedom are frozen out. The potential energy of the ellipsoid in the optical tweezers is [31]

$$U(\theta) = -\frac{V}{2c}[\kappa_x - (\kappa_x - \kappa_y)\sin^2\theta]I_0, \tag{1}$$

where I_0 is the intensity of the trapping laser, $V = 4\pi r_a r_b^2/3$ is the volume of the ellipsoid, c is the speed of light, $\kappa_{x,y} = \alpha_{x,y}/(\epsilon_0 V)$ are the effective susceptibilities of the ellipsoid,

*yinzhangqi@mail.tsinghua.edu.cn

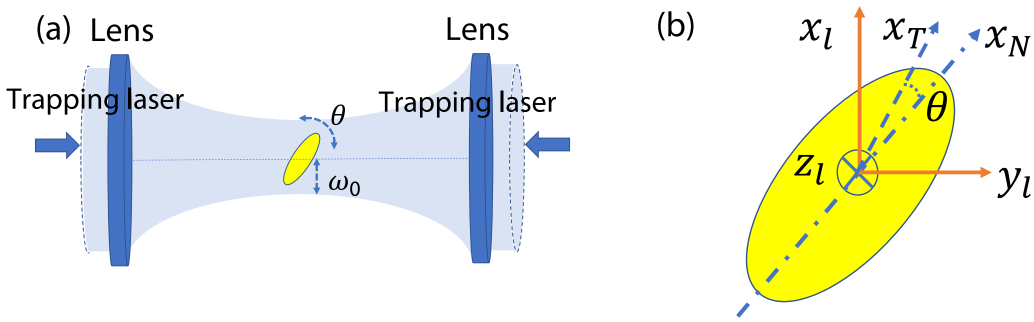

FIG. 1. (a) A schematic diagram of an ellipsoidal nanoparticle trapped by a laser. (b) The relation between the direction of systems of the nanoparticle (x_N), the trapping laser polarization (x_T), and the lens (x_l, y_l, z_l). The x_N axis aligns with the longest axis of the nanoparticle. x_T and x_l axes align with the trapping laser and the center of the two lenses, respectively. The angle between x_N and x_T is θ. The nanoparticle is trapped in a focal plane.

ϵ_0 is the vacuum permittivity, and θ is the angle between the long axis (r_a) of the ellipsoid and the electric field of the laser beam.

The Hamiltonian of the librational mode of this system is

$$H = T + U(\theta), \tag{2}$$

where $T = I\dot{\theta}^2/2$, with $I = 4\pi\rho r_a r_b^2(r_a^2 + r_b^2)/15$ being the rotational inertia of the ellipsoid. By expanding Eq. (2) around the equilibrium position $\theta = 0$ to the fourth order, we get the effective Hamiltonian

$$H = \frac{I\dot{\theta}^2}{2} + \frac{I_0 V(\kappa_x - \kappa_y)}{2c}\theta^2 - \frac{I_0 V(\kappa_x - \kappa_y)}{6c}\theta^4 - \frac{I_0 V \kappa_x}{2c}. \tag{3}$$

We have checked the sixth-order term in the expansion of Eq. (2) and found that it is much smaller than the fourth-order term. Therefore, expanding Eq. (2) to the fourth order is enough for our investigation. With the standard quantization procedure, the Hamiltonian (3) turns into

$$\hat{H}_{\rm mec} = \hat{H}_0 + \hat{H}_1 = \hbar\omega_t^\theta\left(\hat{b}^\dagger\hat{b} + \frac{1}{2}\right) - \hbar\eta(\hat{b}^\dagger + \hat{b})^4,$$

$$\text{with } \omega_t^\theta = \sqrt{\frac{10P_0(\kappa_x - \kappa_y)}{\pi w_0^2 c\rho\left(r_a^2 + r_b^2\right)}}, \quad \eta = \frac{\hbar}{24I}. \tag{4}$$

Here ω_t^θ is the trapping frequency of the librational mode, w_0 is the waist of optical tweezers, and the laser intensity is $I_0 = 2P_0/(\pi w_0^2)$. The librational mode is described by the creation and annihilation operators, $\hat{b}^\dagger$ and $\hat{b}$, which relate to the angle operator $\hat{\theta}$ and the angular momentum $\hat{J}_\theta$ by

$$\hat{\theta} = \frac{\theta_0}{2}(\hat{b} + \hat{b}^\dagger),$$
$$\hat{J}_\theta = \frac{J_0}{2i}(\hat{b} - \hat{b}^\dagger), \tag{5}$$

where $\theta_0 = \sqrt{\frac{2\hbar}{I\omega_t^\theta}}$ and $J_0 = \sqrt{2I\hbar\omega_t^\theta}$.

Equation (4) shows that the nonlinearity of the librational mode is inversely proportional to the inertia of the ellipsoidal nanoparticle, but independent of the power and the shape of the optical trap. The material, size, and shape of the nanoparticle determine the nonlinearity of the librational mode. As shown in Fig. 2(a), the nonlinearity is in inverse proportion to the fifth power of size and in inverse proportion to the density of the particle. Furthermore, the nonlinearity increases with the increment of the eccentricity of the particle with the determined long axis. The shorter long axis and the bigger eccentricity can induce the larger nonlinearity. For example, if the power of laser ($P_0 = 0.1$ W) and the particle's eccentricity ($e = 0.8$) is determined, the ratio between η and ω_t^θ is

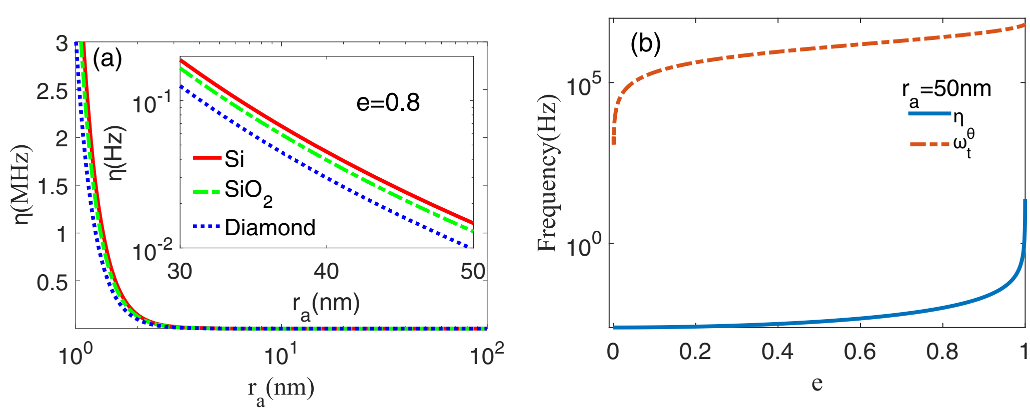

FIG. 2. Nonlinearity versus particle size, material, and eccentricity under the laser power $P_0 = 0.1$ W. (a) The nonlinearity versus long axis ($r_a < 100$ nm) of different material in $e = \sqrt{1 - r_b^2/r_a^2} = 0.8$. The inset shows the nonlinearity for different material. (b) The nonlinearity and the trapping frequency of the diamond particle with different eccentricity, which for the long axis of the nanoparticle is $r_a = 50$ nm.

4.6×10^{-9} (4.6×10^{-5}) for different long axes 50 nm (5 nm). The nonlinearity strength could be on the order of kHz when the long axis of the nanoparticle is around 5 nm. If we reduce the power of the laser to decrease the trapping frequency on the order of 10 kHz, the ratio (η/ω_t^θ) could approach 0.1. As the nonlinearity strength is comparable with the trapping frequency and much larger than the librational mode decay, we may use the librational mode as a qubit. When the long axis is in the region (10,100) nm, the nonlinearity of the librational mode is at least two orders of magnitude larger than the nonlinearity of the center-of-mass mode. A very interesting nonlinear phenomena like bistability may appear in this system.

III. BISTABILITY

Bistability is a ubiquitous phenomena in the nonlinear system. To exhibit the bistable effect, we drive the librational mode of this nonlinear system by a Gaussian laser beam, which linearly polarized at an angle $\pi/4$ with respect to the x axis and modulated by $\sqrt{\cos(\omega_{ml}t)}$ in the directions of x and y. It causes the vibrating amplitude and frequency of particle to be $\Omega = \frac{P_{ml}V(\kappa_x-\kappa_y)}{\pi\omega_0^2 c}\sqrt{\frac{2}{\hbar I\omega_t^\theta}}$ and ω_{ml}, where P_{ml} is the power of the manipulative laser beam. The Hamiltonian of librational mode under drive is

$$\hat{H}_{\text{tot}} = \hat{H}_{\text{mec}} + \hat{H}_{dr},$$
$$\hat{H}_{dr} = \frac{\hbar\Omega}{2}(\hat{b}e^{i\omega_{ml}t} + \hat{b}^\dagger e^{-i\omega_{ml}t}). \tag{6}$$

In the rotating wave frame, the Hamiltonian is transformed following $\hat{H}_{RM} = \hat{U}^\dagger\hat{H}_{\text{tot}}\hat{U} - \hbar\omega_{ml}\hat{b}^\dagger\hat{b}$ and $\hat{U} = e^{-i\omega_{ml}\hat{b}^\dagger\hat{b}t}$,

$$\hat{H}_{RM} = -\hbar\Delta_{ml}\hat{b}^\dagger\hat{b} + \frac{\hbar\Omega}{2}(\hat{b} + \hat{b}^\dagger) - \hbar\eta(\hat{b}e^{i\omega_{ml}t} + \hat{b}^\dagger e^{-i\omega_{ml}t})^4, \tag{7}$$

where $\Delta_{ml} = \omega_{ml} - \omega_t^\theta$ is the detuning between the driving and the trapping laser beams.

The master equation can be used to describe the full dynamics of this nanoparticle, which couples with the thermal bath [48],

$$\dot{\hat{\rho}}(t) = \frac{1}{i\hbar}[\hat{H}_{RM}(t),\hat{\rho}] + \mathscr{L}_b\hat{\rho}, \tag{8}$$

where $\mathscr{L}_b = \frac{(1+\bar{n}_b)}{2}\gamma_b\mathscr{D}_b + \frac{\bar{n}_b}{2}\gamma_b\mathscr{D}_{b^\dagger}$, with the Lindblad operator $\mathscr{D}_x(\rho) = 2x\rho x^\dagger - x^\dagger x\rho - \rho x^\dagger x$. Here γ_b is the decay of librational mode, and $\bar{n}_b$ is the average phonon number of the thermal reservoir.

Using the master Eq. (8), we can deduce the motional equations of the librational mode mean field amplitudes β (β^*):

$$\frac{\partial}{\partial t}\begin{pmatrix}\beta\\ \beta^*\end{pmatrix} = \begin{pmatrix}\left[i\Delta_{ml} - \frac{\gamma_b}{2} + 12i\eta(|\beta|^2+1)\right]\beta - i\frac{\Omega}{2}\\ \left[-i\Delta_{ml} - \frac{\gamma_b}{2} - 12i\eta(|\beta|^2+1)\right]\beta + i\frac{\Omega}{2}\end{pmatrix}. \tag{9}$$

Here we have neglected the highly oscillating terms with frequencies of $\pm 2\omega_{ml}$ and $\pm 4\omega_{ml}$ and applied the semiclassical approximation (i.e., neglecting terms $\langle\hat{b}^\dagger\hat{b}^2\rangle - \langle\hat{b}^\dagger\rangle\langle\hat{b}^2\rangle$), $\langle\hat{b}^\dagger\hat{b}^2\rangle = \beta^*\beta^2$. This approximation requires fluctuation terms $\langle(\delta\hat{b})^2\rangle$ and $\langle\delta\hat{b}^\dagger\delta\hat{b}\rangle$ are much less than $|\beta|^2$. In order to study the stability of the system, the amplitude of librational mode $\beta(t)$ is split into two terms: an average amplitude β_0 and a fluctuation $\beta_1(t)$,

$$\beta(t) = \beta_0 + \beta_1(t), \tag{10}$$

where β_0 is the steady-state solution of Eq. (9), which satisfies

$$\begin{pmatrix}\frac{i\Omega}{2}\\ \frac{-i\Omega}{2}\end{pmatrix} = \begin{pmatrix}\left[i\Delta_{ml} - \frac{\gamma_b}{2} + 12i\eta(n+1)\right]\beta_0\\ \left[-i\Delta_{ml} - \frac{\gamma_b}{2} - 12i\eta(n+1)\right]\beta_0^*\end{pmatrix}. \tag{11}$$

Here $n = |\beta_0|^2$ and the fluctuation β_1 satisfies

$$\frac{\partial}{\partial t}\begin{pmatrix}\beta_1(t)\\ \beta_1(t)^*\end{pmatrix} = -\mathbf{A}\begin{pmatrix}\beta_1(t)\\ \beta_1^*(t)\end{pmatrix}, \tag{12}$$

and

$$\mathbf{A} = \begin{pmatrix}\kappa + 2\chi n & \chi\beta_0^2\\ \chi^*\beta_0^{*2} & \kappa^* + 2\chi^* n\end{pmatrix}. \tag{13}$$

For simplicity, we have defined that $\chi = -12i\eta$ and $\kappa = \gamma_b/2 - i(\Delta_{ml} + 12\eta)$.

In order to obtain stable eigenvalues, we calculate $\text{Tr}(\mathbf{A}) = \gamma_b > 0$ and $\text{Det}(\mathbf{A}) = |\kappa|^2 + 2(\chi\kappa^* + \kappa\chi^*)n + 3|\chi|^2 n^2$. Using the Routh-Hurwitz criterion [49], it is found that Eq. (12) has a steady solution when $\text{Tr}(\mathbf{A}) > 0$ and $\text{Det}(A) > 0$. For the specific n, the Routh-Hurwitz criterion gives stable eigenvalues. The stable condition implies

$$0 \leqslant \omega_{ml} < \omega_t^\theta - 12\eta - \frac{\sqrt{3}\gamma_b}{2}. \tag{14}$$

From Eq. (14), we know that the bistability appears only in the red-detuning ($\Delta_{ml} < 0$) regime, and the blue-detuning drive will not cause bistability. For convenience, we set $\Delta_{\text{eff}} = \Delta_{ml} + 24\eta n$, $\omega_c = \omega_t^\theta - \delta_c$, and $\delta_c = 12\eta(\zeta + 1)$, where $\zeta = \sqrt{3}\gamma_b/24\eta$. If $\omega_{ml} = \omega_t^\theta - 12\eta(\zeta+1) + \delta$, δ varies about ω_c, From Eqs. (11) and (14) we can get

$$\Omega^2 = \left\{\gamma_b^2 + \left[\Delta_{\text{eff}} + \delta - 12\eta(\zeta - 1)\right]^2\right\} \times \frac{\Delta_{\text{eff}} - \delta + 12\eta(\zeta+1)}{24\eta},$$

$$\Delta_{\text{eff}\pm} = \frac{-\delta + 12\eta(\zeta - 3) \pm 2\sqrt{\delta^2 - \sqrt{3}\gamma_b\delta}}{3}. \tag{15}$$

From Eq. (15), we find that when driven frequency (ω_{ml}) is very low, the system needs the strong driven amplitude (Ω) for bistability. However, if the driving frequency is near the resonant frequency, a very weak driving amplitude can also induce bistability. Obviously, the distance between two turning points $\Delta_{\text{eff}\pm}$ is

$$\Delta_w = \Delta_{\text{eff}+} - \Delta_{\text{eff}-} = \frac{4\sqrt{\delta^2 - \sqrt{3}\delta\gamma_b}}{3}, \tag{16}$$

which depends only on detuning and environment. When $\delta = \delta_0 = 12\eta(\zeta - 1) - \Delta_{\text{eff}}$, Ω have the minimum $\gamma_b\sqrt{\frac{\Delta_{\text{eff}}+12\eta}{12\eta}}$. This line is constituted by one turning point of the bistable state, as shown like the point D in Fig. 3. It is easy to know that the output (Δ_{eff}) is the parabola form of driven amplitude

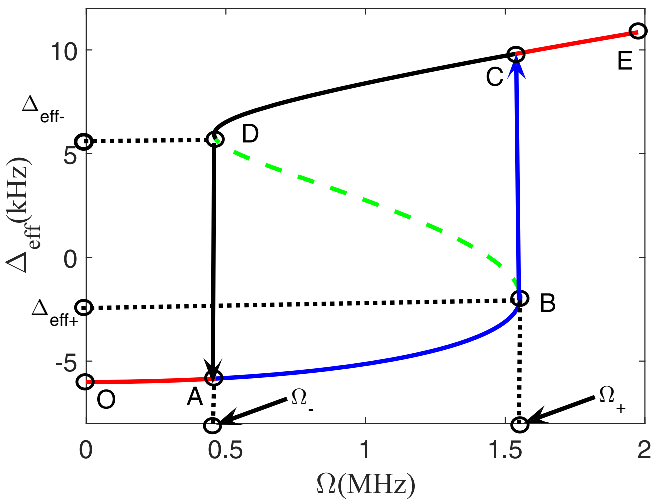

FIG. 3. Bistability of this system in $P = 10$ mTorr. The figure shows the effect of detuning $\Delta_{\rm eff}$ versus driven amplitude Ω. There are several characteristic points, O (0, −6.00 kHz), A (466 kHz, −5.8 kHz), B (1.55 MHz, −1.65 kHz), C (1.55 MHz, 9.86 kHz), D (466 kHz,5.89 kHz), E (2.00 MHz, 10.9 kHz), and the detuning $\omega_{ml} - \omega_t^\theta = -6007$ Hz. The turning points are $B(\Omega_+,\Delta_{\rm eff+})$ and $C(\Omega_-,\Delta_{\rm eff-})$. In this case, the particle with the long axis $r_a = 50$ nm and $e = 0.9$ is trapped by a $P = 0.1$ W and $w_0 = 0.6\ \mu$m laser. The temperature of the system is $T = 300$ K throughout the paper.

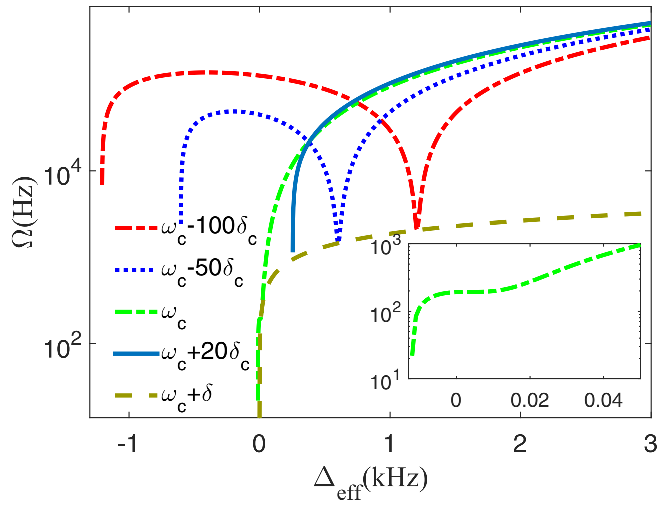

FIG. 4. Bistability of this system for different driving frequency (ω_{ml}). The figure is the driven amplitude Ω versus effect detuning $\Delta_{\rm eff}$. Different colored lines present different driven frequencies in determined resident air pressure $P_{\rm air} = 1\ \mu$Torr. Every line has two extreme value which are the turning points and the distance of them is the bistable window. The inset shows the steady state for the critical driving frequency (ω_c).

(Ω). As a matter of fact, every point in this line is one of the jump points in different bistable state.

The bistability of the librational mode is shown in Fig. 3. The lines OABCE and ECDAO show two stable paths. The dashed line DB is unstable and will not appear in experiments. When $\Delta_{\rm eff}$ increases with the increment of the amplitude (Ω) from O, $\Delta_{\rm eff}$ will jump from B to C in the turning point of B and then increases to E. On the other hand, if Ω decreases from E, $\Delta_{\rm eff}$ should jump down from the turning point D to A with the decrement of Ω and then decrease to O. In brief, the driving frequency (ω_{ml}) determines the system whether happens bistability, and the driving amplitude determines which state the system will go through.

Effective detuning is an important physical quantity. Figure 4 shows the the response of effect detuning ($\Delta_{\rm eff}$) about the driven amplitude (Ω). When $\omega_{ml} < \omega_c$, bistability will appear, and when $\omega_{ml} > \omega_c$, the system has no bistability. When $\omega_{ml} = \omega_c$, a platform will appear as shown in the inset of Fig. 4. The width of the window is determined by detuning the driving frequency. The larger the driving detuning Δ_{ml}, the more the distance Δ_w between two turning points.

If the driven frequency is determined, the relation between Ω and $\Delta_{\rm eff}$ will be affected only by the residual air pressure (P) and temperature (T). For the fixed experimental temperature, the residual air pressure affects only the width of the bistable window. In Fig. 5(a), the width of the window changes little for different P, but the depth is inversely proportional with the air pressure. That is because of the proportional relation between P and γ_b. The larger the decay γ_b, the more energy will be

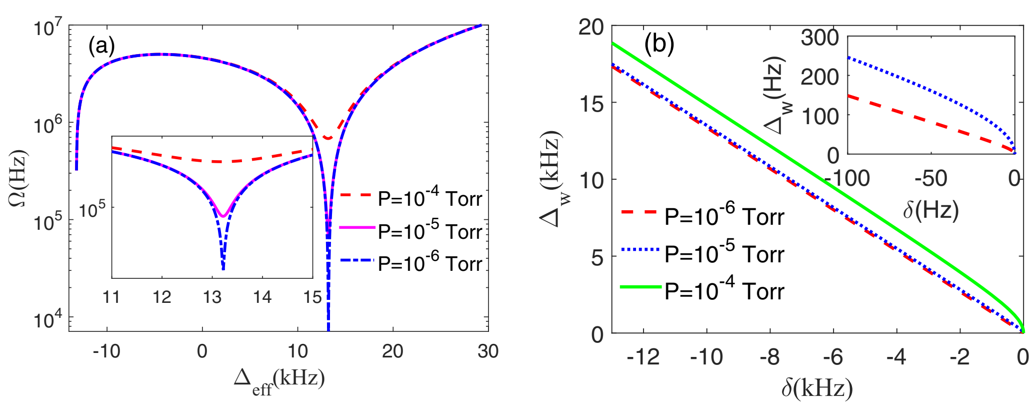

FIG. 5. Bistability of this system and bistable windows in different residual air pressures. (a) Driven amplitude Ω versus detuning $\Delta_{\rm eff}$. Different lines represent different resident air pressures in the determined driven frequency $\omega_{ml} - \omega_t^\theta = -13.26$ kHz. (b) Breadth of bistability Δ_w versus δ. Different lines represent different resident air pressures. The insets are the cases of $P = 10^{-5}$ Torr and $P = 10^{-6}$ Torr.

need for bistability, so the driven amplitude will be bigger. Figure 5(b) shows the relation between the bistable window Δ_w and characteristic detuning δ in different pressure. The higher the air pressure, the larger the window width. When the residual air pressure is very low ($P < 10^{-5}$Torr), the Δ_w will not change anymore. It is worth mentioning that Δ_w is closed when the characteristic detuning is zero.

IV. SQUEEZING

In the last section, we discussed the bistability of the librational mode. Here, we discuss another nonlinearity induced phenomena, librational mode squeezing. In order to generate the squeezed state of the librational mode, we choose the driving detuning and strength to fulfill the stable conditions. By the standard linearization method, we can set $\hat{b} \to \beta_0 + \delta\hat{b}$, β_0 is the steady-state amplitude of the librational mode, and $\delta\hat{b}$ is the fluctuation around the steady state; for simplicity, $\delta\hat{b}$ is written as $\hat{b}$. Therefore, under the rotating wave approximation and setting $\beta_0 = re^{i\phi}$, $r \in \mathbb{R}$ also $|\beta_0| \gg 1$, the linearized Hamiltonian reads

$$\hat{H}_l = -\hbar(\Delta_{ml} + 24\eta r^2)\hat{b}^\dagger\hat{b} - 6\hbar\eta r^2(e^{2i\phi}\hat{b}^{\dagger 2} + \mathrm{e}^{-2i\phi}\hat{b}^2). \tag{17}$$

This Hamiltonian can apply for single-mode squeezing.

Base on Eq. (5), we introduce the Hermitian amplitude operators $\hat{X}_1$ and $\hat{X}_2$, which are essentially dimensionless angle $\hat{\theta}$ and angular momentum $\hat{J}_\theta$ operators, $\hat{X}_1 = \hat{\theta}/\theta_0$ and $\hat{X}_2 = \hat{J}_\theta/J_0$. We define the variances, $\mathcal{S}_\theta = \Delta X_1 = [\langle\hat{\theta}^2\rangle - \langle\hat{\theta}\rangle^2]/\theta_0^2$ and $\mathcal{S}_J = \Delta X_2 = [\langle\hat{J}_\theta^2\rangle - \langle\hat{J}_\theta\rangle^2]/J_0^2$. When $\mathcal{S}_{\theta(J)}$ satisfies the relation

$$\mathcal{S}_{\theta(J)}^2 < \tfrac{1}{4} \tag{18}$$

in the vacuum state, we call $\theta(J_\theta)$ squeezed, which is useful for the precision measurement of angle and angular momentum. We will discuss how to squeeze the thermal and vacuum librational modes.

In experiments, usually, the initial state is not vacuum, but is in the thermal equilibrium. The state of a system with Hamiltonian $\hat{H}$ is represented by the density matrix

$$\hat{\rho}_{th} = \frac{\exp(-\beta_{th}\hat{H})}{\mathrm{Tr}[\exp(-\beta_{th}\hat{H})]}, \tag{19}$$

where $\beta_{th} = (k_B T)^{-1}$, k_B is Boltzmann's constant, and T is temperature. It is well known that the average of the number operator in thermal state is mean thermal phonon number $\bar{n}$. We can use the squeezing Hamiltonian Eq. (17) to generate the thermal squeezing state [50]. The variance of $\hat{X}_1$ and $\hat{X}_2$ in this state will be determined as

$$\mathcal{S}_\theta(t) = \frac{\langle 2\hat{b}^\dagger(0)\hat{b}(0) + 1\rangle}{4\lambda_p^2} \times \{[\xi^2 - \lambda\xi\cos(2\phi)]\sinh(2\lambda_p t) - \lambda\xi\sin(2\phi)\cosh(2\lambda_p t) - [\lambda^2 - \lambda\xi\cos(2\phi)]\}, \tag{20}$$

where $\lambda = \Delta_{ml} + 24\eta r^2$, $\xi = 12\eta r^2$, and $\lambda_p = \sqrt{\xi^2 - \lambda^2}$. Meanwhile, the variance of X_2 evolves as

$$\begin{aligned}\mathcal{S}_J(t) = \Big\{&\big(\xi^4\sin^2(2\phi) + \lambda_p^2\xi^2 - \lambda\xi^3\sin^2(2\phi)\cos(2\phi) + \lambda_p^2\lambda\xi\cos(2\phi) - 2\lambda_p\lambda\xi^2\sin^2(2\phi)\big]\cosh(2\lambda_p t)\\ &- \big[\lambda\xi^2\sin^2(2\phi) + \lambda_p^2\lambda - \lambda_p\xi^2 - \lambda_p\lambda\xi\cos(2\phi)\big] \times \sin(2\phi)\sinh(2\lambda_p t) - \lambda\big[\xi^2\sin^2(2\phi) - \lambda_p^2\big]\\ &\times[\lambda - \xi\cos(2\phi)]\Big\} \times \frac{\langle 2\hat{b}^\dagger(0)\hat{b}(0) + 1\rangle}{4\lambda_p^2(\xi\cos(2\phi) - \lambda)^2}.\end{aligned} \tag{21}$$

Here, the average of $\langle\hat{b}^\dagger(0)\hat{b}(0)\rangle$ is the mean thermal phonon number $\bar{n}$. We can determine whether $\Delta X_i (i = 1,2)$ is squeezed in thermal state by [50]

$$(\Delta X_i)^2 < \tfrac{1}{4}(2\bar{n} + 1). \tag{22}$$

By using the squeezed thermal state, we may increase the measurement precision on either angle or angular momentum without cooling the system. If the system is in the vacuum state ($\langle\hat{b}^\dagger(0)\hat{b}(0)\rangle = 0$) at the initial time, this situation will reduce to Eq. (18).

It is easy to know that the formation of λ_p decides the property of $\mathcal{S}_\theta$; now we must analyze the property of λ_p. The system has two characteristic points, $\omega_{ml1} = \omega_t^\theta - 36\eta r^2$ and $\omega_{ml2} = \omega_t^\theta - 12\eta r^2$. First, we consider $\omega_{ml1} < \omega_{ml} < \omega_{ml2}$, where $\lambda_p \in \mathbb{R}$ and $\lambda_p > 0$. In this case, we can define $\cos(\arctan\frac{\lambda_p}{\lambda}) = \frac{\lambda}{\sqrt{\lambda^2+\lambda_p^2}}$ and $\sin(\arctan\frac{\lambda_p}{\lambda}) = \frac{\lambda_p}{\sqrt{\lambda^2+\lambda_p^2}}$, and Eq. (20) can simplify as follows:

$$\begin{aligned}\mathcal{S}_\theta = \frac{\xi^2}{4(\xi^2 - \lambda^2)} \times \Bigg\{&\left[1 - \cos\left(2\phi - \arctan\frac{\lambda_p}{\lambda}\right)\right]e^{2\lambda_p t}\\ &+ \left[1 - \cos\left(2\phi + \arctan\frac{\lambda_p}{\lambda}\right)\right]e^{-2\lambda_p t}\\ &+ 2\frac{\lambda}{\xi}\left[\cos(2\phi) - \frac{\lambda}{\xi}\right]\Bigg\}.\end{aligned} \tag{23}$$

For different squeezing angle, we have different squeezing of variance $\mathcal{S}_\theta$ as follows:

$$\mathcal{S}_\theta = \begin{cases}\frac{1}{4}e^{-2\lambda_p t} & \phi = \frac{1}{2}\arctan(\frac{\lambda_p}{\lambda}) + n\pi,\\ \frac{1}{4}e^{2\lambda_p t} & \phi = n\pi - \frac{1}{2}\arctan(\frac{\lambda_p}{\lambda}).\end{cases} \tag{24}$$

It is easy to know that when $\phi = \frac{1}{2}\arctan(\frac{\lambda_p}{\lambda}) + n\pi$, $\mathcal{S}_\theta$ will decrease to zero in a particular direction, which presents that the fluctuation of θ will be zero and the measurement accuracy is very high, and λ_p determines the speed of decay. Namely, Δ_{ml} and ηr^2 codetermine the decay speed. At the same time, another direction will increase undoubtedly.

The second case is $\omega_{ml} < \omega_{ml1}$ or $\omega_{ml} > \omega_{ml2}$. Obviously, $\lambda_p^2 < 0$, so $\lambda_p = \pm i\lambda_p'$ and $\lambda_p' = \sqrt{(\omega_{ml} - \omega_{ml1})(\omega_{ml} - \omega_{ml2})} > 0$, the squeezing of the variance of $\hat{X}_1$ will be

$$\mathcal{S}_\theta = \frac{1}{4\lambda_p^2} \times \Big\{\xi\big[\xi - \lambda\cos(2\phi)\big]\cos(2\lambda_p' t) + \xi\lambda_p'\sin(2\phi)\sin(2\lambda_p' t) + \lambda\big[\xi\cos(2\phi) - \lambda)\big]\Big\}. \tag{25}$$

It is the same with the last section; different squeezing direction will give different variance squeezing. In some direction, the librational mode is amplified; for example, $\phi = \frac{\pi}{2} + m\pi$.

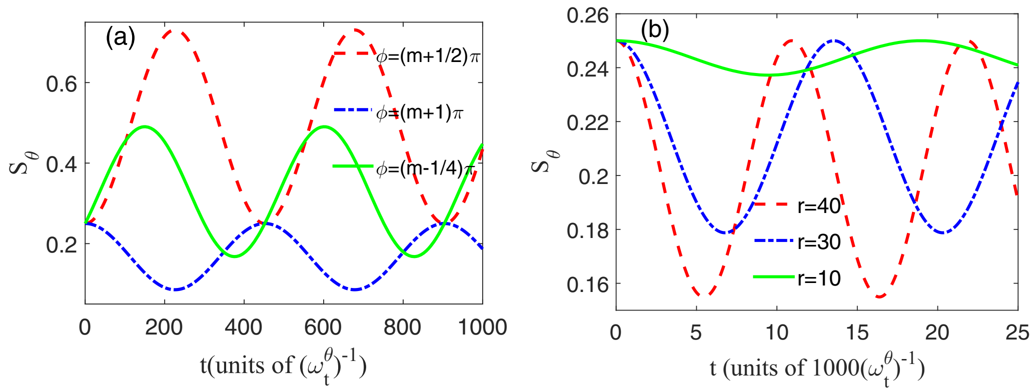

FIG. 6. The oscillatory squeezing of the librational mode. The abscissas are respectively in units of the oscillatory period and the 1000 times oscillatory period of the librational mode. The oscillatory period of the librational mode is 0.79 μs. (a) Different variance squeezing of different direction in oscillation and $r = 40$. These lines denote different squeezing direction. (b) The oscillation squeezing X_1 of the direction of $\phi = (n+1)\pi$ in different r. Different lines represent the behaviors of different oscillatory squeezing in different squeezing amplitudes. In this case, $r_a = 50$ nm, $r_b = 40$ nm, $\omega_t^\theta = 1.2621$ MHz, and $\omega_{ml} - \omega_t^\theta = 0.2$ kHz.

However, the librational mode is oscillatorily squeezed in $\phi = \pi + m\pi$, and the others are the result of joint action of the amplification and squeezing. Their oscillatory periods are the same, π/λ'_p:

$$\mathcal{S}_\theta = \begin{cases} \frac{1}{4} - \frac{3\eta r^2}{\Delta_{ml}+24\eta r^2}\sin(2\lambda'_p t) & \phi = \frac{1}{2}\arccos(\frac{\xi}{\lambda}), \\ \frac{1}{4} + \frac{3\eta r^2}{\Delta_{ml}+12\eta r^2}[1-\cos(2\lambda'_p t)] & \phi = \frac{\pi}{2} + m\pi, \\ \frac{1}{4} + \frac{3\eta r^2}{\Delta_{ml}+36\eta r^2}[\cos(2\lambda'_p t) - 1] & \phi = \pi + m\pi, \\ \frac{1}{4} - \frac{\xi\sin(\lambda'_p t)}{2(\xi^2-\lambda^2)}[\xi\sin(\lambda'_p t) \mp \lambda'_p\cos(\lambda'_p t)] & \phi = \pm\frac{\pi}{4} + m\pi. \end{cases} \tag{26}$$

In order to explain more clearly, we plot Fig. 6. From Fig. 6(a), when the squeezing phase angle is $\phi = (m+1)\pi$, the squeezing ratio of $\hat{X}_1$ is always less than 0.25; namely, the metrical uncertainty of the librational angle is decreased. However, the other direction does not fully present the squeezing property. Therefore, in some direction we can measure always more accurately about X_1 or θ like $\phi = (m+1)\pi$ in Figs. 6(a) and 6(b); on the contrary, the measurement of angular momentum is not so accurate.

At the same time, a different squeezing amplitude can induce a different squeezing ratio and squeezing oscillating period in the certain squeezing direction. For example, in the direction of $\phi = (m+1)\pi$, the squeezing ratio and the squeezing oscillating period is determined by the driving frequency (ω_{ml}) and the squeezing amplitude (r). The bigger squeezing amplitude causes the larger squeezing ratio; furthermore, the squeezing oscillating period is smaller, as shown in Fig. 6(b).

V. CONCLUSION

We have systematically investigated the nonlinearity and related phenomenon of the librational mode of an optically levitated ellipsoidal nanoparticle. By utilizing a quantization method, we have found the nonlinearity of the librational mode is independent of the frequency and power of the laser, and it is only inversely proportional with the rotational inertia of the particle. The nonlinearity of the librational mode is at least two orders larger than the center-of-mass mode of ellipsoidal nanoparticle. In order to generate the squeezed states for librational mode, we bring a drive to it and find different driving amplitudes and frequencies can stimulate different steady states. Red-detuning driving induces bistability, but the system is always stable when the driving is blue detuning. In the stable region, by properly tuning the driving detuning and the strength, we can squeeze the variance of the angle operator in a certain direction, which is useful for the precise measurement of the angle and the angular momentum. In the future, we plan to study how to induce the strong coupling between the librational and the translational modes by proper external driving [51]. It would be useful for quantum information processing and sympathetic cooling.

ACKNOWLEDGMENTS

We thank Tongcang Li and Lei-Ming Zhou for helpful discussions. This work is supported by the National Natural Science Foundation of China under Grants No. 61435007 and No. 11374032, the Joint Fund of the Ministry of Education of China under Grants No. 6141A02011604, NSAF (China) under Grants No. U1530401, and National Key Research and Development Program of China under Grants No. 2016YFA0301201.

[1] M. Aspelmeyer, T. J. Kippenberg, and F. Marquardt, Rev. Mod. Phys. **86**, 1391 (2014).
[2] T. Kippenberg and K. Vahala, Opt. Express **15**, 17172 (2007).
[3] G. Ranjit, D. P. Atherton, J. H. Stutz, M. Cunningham, and A. A. Geraci, Phys. Rev. A **91**, 051805 (2015).
[4] G. Ranjit, M. Cunningham, K. Casey, and A. A. Geraci, Phys. Rev. A **93**, 053801 (2016).
[5] D. C. Moore, A. D. Rider, and G. Gratta, Phys. Rev. Lett. **113**, 251801 (2014).
[6] A. D. Rider, D. C. Moore, C. P. Blakemore, M. Louis, M. Lu, and G. Gratta, Phys. Rev. Lett. **117**, 101101 (2016).
[7] G. Volpe and D. Petrov, Phys. Rev. Lett. **97**, 210603 (2006).
[8] F. Pedaci, Z. Huang, M. van Oene, S. Barland, and N. H. Dekker, Nat. Phys. **7**, 259 (2010).
[9] A. Albrecht, A. Retzker, and M. B. Plenio, Phys. Rev. A **90**, 033834 (2014).
[10] A. Bassi and G. Ghirardi, Phys. Rep. **379**, 257 (2003).
[11] X. Zhang and A. M. Armani, Opt. Express **21**, 23592 (2013).
[12] G. Anetsberger, O. Arcizet, Q. P. Unterreithmeier, R. Rivière, A. Schliesser, E. M. Weig, J. P. Kotthaus, and T. J. Kippenberg, Nat. Phys. **5**, 909 (2009).
[13] M. L. Gorodetsky and V. S. Ilchenko, J. Opt. Soc. Am. B **16**, 147 (1999).
[14] O. Romero-Isart, M. L. Juan, R. Quidant, and J. I. Cirac, New J. Phys. **12**, 033015 (2010).
[15] D. E. Chang, C. A. Regal, S. B. Papp, D. J. Wilson, J. Ye, O. Painter, H. J. Kimble, and P. Zoller, Proc. Natl. Acad. Sci. USA **107**, 1005 (2010).
[16] T. Li, S. Kheifets, and M. G. Raizen, Nat. Phys. **7**, 527 (2011).
[17] T. Li, S. Kheifets, D. Medellin, and M. G. Raizen, Science **328**, 1673 (2010).
[18] V. Jain, J. Gieseler, C. Moritz, C. Dellago, R. Quidant, and L. Novotny, Phys. Rev. Lett. **116**, 243601 (2016).
[19] Z.-q. Yin, A. A. Geraci, and T. Li, Int. J. Mod. Phys. B **27**, 1330018 (2013).
[20] G. Volpe, G. Volpe, and D. Petrov, Phys. Rev. E **76**, 061118 (2007).
[21] N. Zhao and Z.-q. Yin, Phys. Rev. A **90**, 042118 (2014).
[22] O. Romero-Isart, A. C. Pflanzer, F. Blaser, R. Kaltenbaek, N. Kiesel, M. Aspelmeyer, and J. I. Cirac, Phys. Rev. Lett. **107**, 020405 (2011).
[23] Z. Q. Yin, T. Li, X. Zhang, and L. M. Duan, Phys. Rev. A **88**, 033614 (2013).
[24] O. Romero-Isart, Phys. Rev. A **84**, 052121 (2011).
[25] Z.-q. Yin and T. Li, Contemp. Phys. **58**, 119 (2017).
[26] J. Millen, P. Z. G. Fonseca, T. Mavrogordatos, T. S. Monteiro, and P. F. Barker, Phys. Rev. Lett. **114**, 123602 (2015).
[27] J. Gieseler, B. Deutsch, R. Quidant, and L. Novotny, Phys. Rev. Lett. **109**, 103603 (2012).
[28] M. Bhattacharya and P. Meystre, Phys. Rev. Lett. **99**, 153603 (2007).
[29] L.-M. Zhou, K.-W. Xiao, J. Chen, and N. Zhao, Laser Photonics Rev. **11**, 1600284 (2017).
[30] H. Shi and M. Bhattacharya, J. Mod. Opt. **60**, 382 (2013).
[31] T. M. Hoang, Y. Ma, J. Ahn, J. Bang, F. Robicheaux, Z.-Q. Yin, and T. Li, Phys. Rev. Lett. **117**, 123604 (2016).
[32] S. Kuhn, A. Kosloff, B. A. Stickler, F. Patolsky, K. Hornberger, M. Arndt, and J. Millen, Optica **4**, 356 (2017).
[33] B. A. Stickler, B. Papendell, and K. Hornberger, Phys. Rev. A **94**, 033828 (2016).
[34] C. Zhong and F. Robicheaux, Phys. Rev. A **94**, 052109 (2016).
[35] Y. Ma, T. M. Hoang, M. Gong, T. Li, and Z.-q. Yin, arXiv:1611.05599.
[36] T. Delord, L. Nicolas, Y. Chassagneux, and G. Hétet, arXiv:1702.00774.
[37] N. Zhao, D.-l. Zhou, and J.-l. Zhu, Commun. Theor. Phys. **50**, 1457 (2008).
[38] J. Gieseler, L. Novotny, and R. Quidant, Nat. Phys. **9**, 806 (2013).
[39] J. Gieseler, M. Spasenović, L. Novotny, and R. Quidant, Phys. Rev. Lett. **112**, 103603 (2014).
[40] G. Brawley, M. Vanner, P. E. Larsen, S. Schmid, A. Boisen, and W. Bowen, Nat. Commun. **7**, 10988 (2016).
[41] X.-Y. Lü, J.-Q. Liao, L. Tian, and F. Nori, Phys. Rev. A **91**, 013834 (2015).
[42] J.-Q. Liao and F. Nori, Phys. Rev. A **88**, 023853 (2013).
[43] C. Zhu, L. Dong, and H. Pu, Phys. Rev. A **94**, 053621 (2016).
[44] A. L. Grimsmo and A. S. Parkins, J. Phys. B: At., Mol. Opt. Phys. **46**, 224012 (2013).
[45] J. Fan, C. Huang, and L. Zhu, Opt. Express **23**, 2973 (2015).
[46] P. Z. G. Fonseca, E. B. Aranas, J. Millen, T. S. Monteiro, and P. F. Barker, Phys. Rev. Lett. **117**, 173602 (2016).
[47] P. Huang, J. Zhou, L. Zhang, D. Hou, S. Lin, W. Deng, C. Meng, C. Duan, C. Ju, and X. Zheng, Nat. Commun. **7**, 11517 (2016).
[48] W. H. Louisell and W. H. Louisell, *Quantum Statistical Properties of Radiation* (Wiley, New York, 1973), Vol. 7.
[49] E. X. DeJesus and C. Kaufman, Phys. Rev. A **35**, 5288 (1987).
[50] M. Rashid, T. Tufarelli, J. Bateman, J. Vovrosh, D. Hempston, M. S. Kim, and H. Ulbricht, Phys. Rev. Lett. **117**, 273601 (2016).
[51] S. Liu, T. Li, and Z. qi Yin, J. Opt. Soc. Am. B **34**, C8 (2017).